Journal of the Optical Society of America B
OPTICAL PHYSICS

Metasurface-enhanced optical Tamm states and related lasing effect

Zhenqing Zhang,[1] Yunhui Li,[1,*] Shaohua Wang,[1] Hai Lu,[2] Yong Sun,[1] Haitao Jiang,[1] and Hong Chen[1]

[1]MOE Key Laboratory of Advanced Micro-Structured Materials, School of Physics Science and Engineering, Tongji University, Shanghai 200092, China
[2]College of Physics and Electronic Engineering, Henan Normal University, Xinxiang 453007, China
*Corresponding author: liyunhui@tongji.edu.cn

Received 16 March 2015; revised 4 June 2015; accepted 4 June 2015; posted 19 June 2015 (Doc. ID 236201); published 14 July 2015

In this paper, meta-surface with electromagnetically induced-reflection-like (EIR-like) dispersion is introduced to enhance the optical Tamm state (OTS) and related lasing effect. Numerical analysis and full-wave simulation confirm that this structure-induced EIR-like dispersion of meta-surface gives rise to the *Q*-factor of OTS. Consequently, enhanced lasing effect also is investigated when a four-level two-electron atomic system is introduced. The results show that the lasing threshold can almost be reduced to half, with the enhancement of max emission intensity in the mean time. These features make the meta-surface-enhanced OTS structure promising for reducing the lasing threshold, enhancing the fluorescence, and so on.

OCIS codes: (140.3945) Microcavities; (160.3918) Metamaterials; (160.5298) Photonic crystals; (240.6680) Surface plasmons; (240.6700) Surfaces.

http://dx.doi.org/10.1364/JOSAB.32.001624

1. INTRODUCTION

Recent investigations have shown that there are optical Tamm states (OTSs) existing at the interface of a metal-photonic crystal (M-PC) hetero-structure [1,2]. Unlike conventional surface plasmon polaritons (SPPs) on a metal surface, OTSs can be excited directly by normally incident propagating waves for both TE and TM polarizations. Owing to strong electromagnetic localization around the interface, potential applications of OTSs have been proposed in recent years, such as polariton lasers [3], enhancement of Faraday rotation [4], and various nonlinear effects [5,6].

To understand more explicitly the propagating behavior of EM waves in the M-PC hetero-structures, OTSs also can also analogous with the tunneling modes in a pair of slabs: one is an epsilon-negative (ENG) layer and the other a mu-negative (MNG) one. In 2003, Alù and Engheta pointed out that [7] under the matching condition EM waves tend to tunnel through the hetero-structure made of ENG and MNG, despite their evanescent nature in the individual ENG or MNG layer. The whole structure hereby becomes transparent at the tunneling frequency, with a strong localized EM field at the interface of the hetero-structure.

In optical frequency range, a metal slab or metallic meta-surface, used to form the OTSs in metal-PC or meta-surface-PC (MS-PC) hetero-structure, can be regarded as a type of epsilon-negative material below its plasma frequency, while PC, taking advantage of its stop band properties, is thought to be equivalent to an SNG, particularly a MNG, effective material under some well-engineered geometric and electromagnetic parameters. Under the matching condition, a light tunneling effect can occur within the hetero-structure consisting of metal (or metallic meta-surface) and photonic crystal, which is also understood as the OTS.

For better modulation of the electromagnetic (EM) tunneling effect of OTSs, some metallic structures, such as microdisks [8] or meta-atoms with electromagnetically induced-reflection-like (EIR-like) properties [9], are patterned on the thin metal layer of the hetero-structure. From our point of view, both of these two methods reconfigure the EM response of the patterned metallic layer, namely, the meta-surface, into a highly dispersive one. Intriguingly, these methods provide extra and wide freedom of tuning the EM wave propagating behavior within the hetero-structure, such as transmission, *Q*-factor, and even the local density of optical states (LDOS) that dominates the related nonlinear or plasmon lasing phenomena.

As is known, types of meta-surfaces exhibiting amazing power to control the light flow have been proposed recently. These include manipulating the light polarization [10], presenting photonic spin hall effect [11], achieving three-dimensional optical holography [12], and so on. However, here we mainly focus on their highly dispersive property originating from some quantum-like interference effects. For instance,

various quantum optical phenomena, including EIR and related electromagnetically induced transparency (EIT), are mimicked in the classical systems based on "meta-atom" or "meta-molecular" [13–16]. In 2008, a plasmonic analogy of EIT was proposed by Zhang and co-workers [14], etc., exhibiting typical EIT-like properties, for instance, slow light, steep phase dispersion, and spatial localization of light. Soon after, some theoretical and experimental works in different systems also were carried out to demonstrate the EIT-like effect by Tassin *et al.* [15]. Compared to cold atomic gas, usually in terms of three-level quantum optical systems, this sort of solid-state-based configuration is more stable, low cost, and easily integrated. Specially, instead of an EIT-like transmission window, similar EIT-like reflectance spectra also can be obtained in complementary planar metamaterials, which is the so-called electromagnetically induced-reflection [16]. Because of the coupling between different "meta-atoms" etched on a thin metal film, tiny "hot-spots" with highly localized electromagnetic (EM) fields can be created. It also has been found that these complementary planar metamaterials possessing narrow reflectance peaks are crucial for the application of plasmonic sensing. However, the EM confinement for these structures is determined only by the in-plane coupling between adjacent "dark" and "bright" meta-atoms. To enhance the EM localization further, confinement along the propagating direction of EM waves also may be involved.

In this paper, enhanced OTSs and the related lasing effect in a meta-surface-PC (MS-PC) hetero-structure are investigated intensively. The meta-surface is consisting of periodically patterned "meta-molecules" on the thin metal layer. By adjusting the coupling between bright and dark "meta-atoms" in a unit cell, EIR-like dispersion can be achieved, which makes the properties of hetero-structure more tunable. After that, one-dimensional PCs composed of TiO_2/SiO_2 are also designed properly to satisfy the matching condition of OTS in the MS-PC hetero-structure. First, analysis based on the transfer matrix method (TMM) is performed to verify the Q-factor enhancement effect occurring in an ENG-MNG hetero-structure. It is clear that by engineering the dispersion of ENG metamaterials, for instance, employing a structure-induced EIR-like dispersion, Q-factor for the hetero-structure is boosted efficiently; that is, the patterned meta-atoms dramatically modify the dispersion of metal layer that is regarded as the ENG materials in optics, resulting in the Q-factor enhancement. Compared with traditional methods that change mainly the MNG part of the hetero-structure, i.e., the PCs, no extra device volume would be added. Next, by embedding gain materials into the hotspots, stronger light amplification and lower lasing threshold are observed clearly. In our case, a detailed four-level, two-electron atomic system is also hired to describe the gain materials, which makes our results closer to those in a realistic lasing system. Full-wave EM simulations based on finite-difference time-domain (FDTD) are carried out to verify the enhanced OTSs and related lasing effect. The results show that the lasing threshold almost can be reduced to half, with the enhancement of max emission intensity in the mean time. Thus, we demonstrate that our structure of a MS-PC hetero-structure is promising to further lower the threshold of plasmonic lasers.

2. NUMERICAL ANALYSIS

A. Analytic Method

First, we briefly analyze the tunneling conditions when an electromagnetic wave propagates in an ENG and MNG hetero-structure. The ENG and MNG hetero-structures are formed by two layers of electromagnetic materials. Their corresponding permittivity, permeability, and thickness are ε_1, μ_1, d_1 and ε_2, μ_2, and d_2, as shown in Fig. 1.

A Drude model is used to describe the permittivity and permeability of the ENG and MNG [17] hetero-structures:

$$\varepsilon_1 = 1 - \frac{\alpha_\varepsilon^2}{(\omega^2 + i\beta_\varepsilon\omega)} \tag{1a}$$

$$\mu_2 = 1 - \frac{\alpha_\mu^2}{(\omega^2 + i\beta_\mu\omega)} \tag{1b}$$

where $d_1 = 80$ nm, $d_2 = 80$ nm, $\alpha_\varepsilon = \alpha_\mu = 6 \times 10^{15}$ Hz, $\beta_\varepsilon = \beta_\mu = 5 \times 10^{12}$ Hz, and $\mu_1 = \varepsilon_2 = 3$.

Meanwhile, the permittivity and the permeability of the left environment area are supposed to be ε_{in} and μ_{in}, while those for the right one are ε_{out} and μ_{out}.

The transmission spectrum can be plotted out by the TMM [18]. The tunneling conditions in the ENG and MNG hetero-structure can be described as follows [7]:

$$\begin{cases} \frac{\varepsilon_1(\omega)d_1+\varepsilon_2 d_2}{d_1+d_2} = \varepsilon_{\text{eff}} = 0 \\ \frac{\mu_1 d_1+\mu_2(\omega)d_2}{d_1+d_2} = \mu_{\text{eff}} = 0 \end{cases} \tag{2}$$

In Fig. 2, it is obvious that a transmission peak (black dashed line) appears at $f = 477.3$ THz for the hetero-structure consisting of ENG and MNG metamaterials whose dispersion adopts a form of Drude model.

To present the above electromagnetic tunneling phenomenon in the visible light range, two kinds of SNG with Drude-like dispersion have to be realized. Relatively, it is easy to realize ENG in optical frequency range. In nature, a variety of metals, below their plasma oscillation frequency, have a negative dielectric response with Drude-like dispersion, which makes them effective ENG metamaterials. Nevertheless, it is not convenient to achieve MNG with Drude-like dispersion in an optical band. Although different types of optical magnetic metamaterials have been proposed, such as the split ring resonator and the fishnet structure, their dispersion of permeability is always

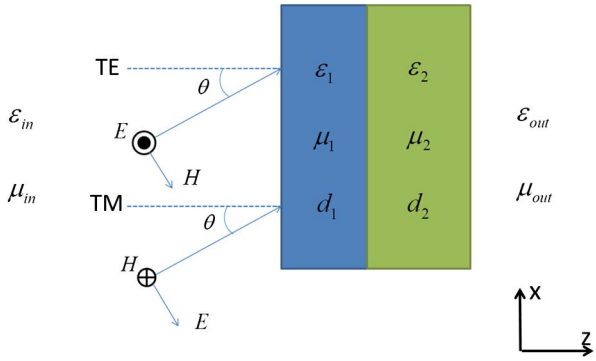

Fig. 1. Schematic of an ENG and MNG hetero-structure.

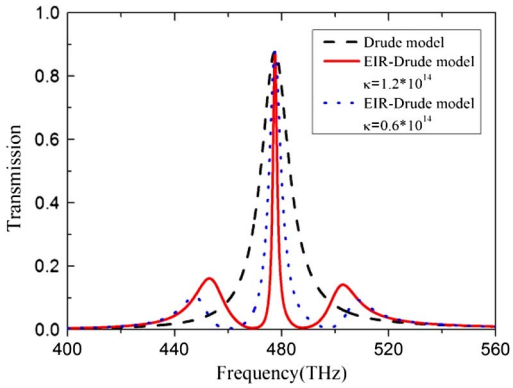

Fig. 2. Transmission spectra of the ENG and MNG hetero-structure whose ENG part adopts a Drude model (black dashed line), EIR-Drude model with different κ values (blue dotted and red solid line), respectively.

in the form of a Lorentz model. As a result, the frequency range of negative permeability is so narrow that it is difficult to match up with the ENG metamaterials and realize the electromagnetic tunneling. It is also found that a well-engineered, one-dimensional PC with a specific band gap could be regarded as a MNG metamaterial with Drude-like dispersion [19]. Therefore, the electromagnetic tunneling phenomenon, namely, the OTS, can be realized optically by using the metal-PC hetero-structure.

Observing the above tunneling conditions carefully, one can understand intuitively that previous adjustment of the OTS transmission properties is achieved mainly by modifying the magnetic part of the above condition, in particular, the $\mu_{2(\omega)}$. Practical means include changing the refractive index of the material, the period length, and the period number of the one-dimensional PC. Unfortunately, the value range of the material refractive index in nature is restricted, while the increased number of periods will certainly expand the device volume. Therefore, to some degree, these traditional modulating methods still have some limitations.

Instead of changing the dispersion of one-dimensional PC $\mu_{2(\omega)}$, we found that the transmission properties of OTS can also be fine-tuned by properly varying the dispersion of the metal layer $\varepsilon_{1(\omega)}$. It is found that, by patterning on some well-designed artificial structures, the thin metallic layer turns out to be a meta-surface with *structure-induced* dispersion. Now, the permittivity of ENG can be redesigned by adding an EIR-like dispersion into Eq. (1a), which makes it become [14]

$$\begin{cases} \varepsilon_1 = 1 - \frac{\alpha_\varepsilon^2}{(\omega^2 + i\beta_\varepsilon\omega)} + \chi(\omega) \\ \chi(\omega) = -\frac{h(\omega-\omega_0+i\gamma_b)}{(\omega-\omega_0+i\gamma_a)(\omega-\omega_0+i\gamma_b)-\kappa^2} \end{cases} \quad \textbf{(3a)}$$

$$\mu_2 = 1 - \frac{\alpha_\mu^2}{(\omega^2 + i\beta_\mu\omega)}, \quad \textbf{(3b)}$$

where ω_0 is the resonant angular frequency of the radiative and dark resonators; γ_a and γ_b are the damping factors of the two resonators; κ indicates the coupling between the two resonators; and h is a geometric parameter indicating the strength of the radiative element couples with the incident electromagnetic wave. Other parameters are

$$\alpha_\varepsilon = \alpha_\mu = 6\times10^{15}\ \text{Hz}; \quad \beta_\varepsilon = \beta_\mu = 5\times10^{12}\ \text{Hz};$$
$$\mu_1 = \varepsilon_2 = 3 \quad \gamma_a = 5\times10^{13}\ \text{Hz}; \quad \gamma_b = 1\times10^{8}\ \text{Hz};$$
$$\kappa = 6\times10^{13}\ \text{Hz}; d_1 = 80\ \text{nm}, \quad d_2 = 80\ \text{nm},$$
$$h = 1\times10^{14}\ \text{Hz}.$$

When an EIR-like dispersion is superimposed to the original Drude model, the transmission spectrum for different κ values (blue dotted and red solid line) also can be replotted by TMM in Fig. 2. In the following paragraph, we named this composite dispersion as the EIR-Drude model. It shows obviously that the Q-factor of the OTS mode is enhanced greatly while the transmission is unchanged. In the meantime, the Q-factor is enhanced along with the decrease of meta-atoms' coupling strength κ value in permittivity of ENG. This result implies that the transmission properties, in particular the Q-factor of the ENG-MNG hetero-structure, can be well engineered by introducing EIR-like dispersion into the original ENG metamaterials.

B. Parameter Retrieval of Meta-Surface with EIR-like Dispersion Method

Above we have verified analytically that the employed EIR-like dispersion can give rise to the Q-factor of the tunneling mode effectively. Next, we would like to discuss the realization of ENG with extra EIR-like dispersion by full-wave simulations of a feasible meta-surface structure, shown in Fig. 3(a).

By a parameter retrieval method, we can obtain the effective permittivity and permeability of the meta-surface from its reflection and transmission coefficients [18]. Two horizontal and one vertical air slots, regarded as the dark and bright meta-atoms, are etched on the thin metal layer to mimic the

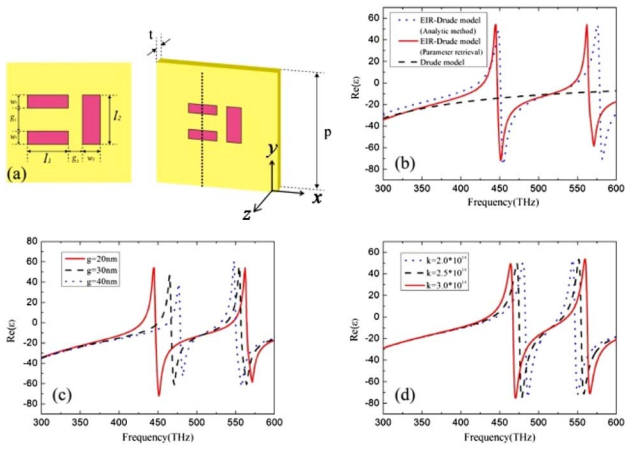

Fig. 3. (a) Schematic of a meta-surface with EIR-like dispersion: top (left panel) and side views (right one). (b) The real parts of permittivity of the Drude dispersion (black dashed line), the EIR-Drude dispersion (blue dashed line), and the retrieved parameters from the simulation on a meta-surface with EIR-like dispersion (red solid line). (c) The real parts of permittivity for a meta-surface with EIR-like dispersion under different g_2. (d) The real parts of permittivity for an EIR-Drude model under different coupling strength κ.

EIR-like phenomenon [16]. The structural parameters are designed as $l_1 = 100$ nm, $w_1 = 30$ nm, $g_1 = 60$ nm, $l_2 = 128$ nm, $w_2 = 50$ nm, $g_2 = 20$ nm, $t = 30$ nm, and $s = 400$ nm. From the simulated reflection and transmission coefficients, we can obtain the effective permittivity of the meta-surface, depicted as the red solid line in Fig. 3(b). For comparison, the dispersive effective permittivity of bulky silver described by the Drude model and that of the above mentioned EIR-Drude model are both shown in Fig. 3(b) as the black dashed line and the blue dotted one, respectively. It is clear that the retrieved dispersion of a realistic meta-surface possessing an EIR-like spectrum agrees well with the analytical EIR-Drude model.

To reveal further the relationship between the well-designed meta-surface and the EIR-Drude model, comparisons under a set of parameters are carried out. In more specific terms, the dispersions of the realistic meta-surface structures with various g_2, the distance between two horizontal slots and a vertical one, are figured out as shown in Fig. 3(c). This changing of g_2 can be understood as the tuning of the coupling between two horizontal slots and a vertical one, namely, the coupling between dark and bright meta-atoms. One can find that this kind of change in a real structure has almost the same impact as that in the EIR-Drude model when varying the coupling parameters κ, which narrows the spectrum width notably. As shown in Fig. 3(d), it is clear that tuning the coupling parameters κ makes the dispersion of an EIR-Drude model changing with the same trends as in Fig. 3(c). Here, g_2 varies from 20 to 40 nm, while κ varies from 3×10^{14} to 2×10^{14} Hz, accordingly, under the condition that $h = 5 \times 10^{14}$ Hz, $\gamma_a = 3 \times 10^{13}$ Hz, and $\gamma_b = 1 \times 10^{8}$ Hz.

Therefore, based on the analysis above, if one redesigns the dispersion characteristics of $\varepsilon_1(\omega)$ by etching an air slot on the thin metal layer to introduce extra EIR-like dispersion, one can further modify or enhance the spectral properties of OTSs, including reflection and Q-factor. Moreover, this enhancement is not at the cost of extra device volume. According to Ref. [9], EM waves are highly localized in the air slot with a maximum E-field strength about two orders higher than conventional OTS hetero-structures, by introducing extra like-EIR dispersion. More importantly, EM fields are found highly localized in the air slot, giving rise to the interaction between light and active materials. Thus, this feature is expected to be applied in the enhancement of lasing behavior.

It should be noticed that, as the EM fields are highly localized around the EIR-like meta-molecule, the adjacent dielectric environment should be taken into account when a parameter retrieval method is performed. For instance, we hire a TiO_2 layer with its thickness of d as a substrate and plot the reflection coefficients in Fig. 4(a).

One can find that the EIR-like spectrum obviously shifts to lower frequency along with the increased substrate thickness d. However, the shifting rate gradually decreases around the lower frequency range. These features imply that, as the EM field is strongly localized around an EIR-like meta-molecule, it cannot influence a substrate that is thick enough. To present it more clearly, we show the EM field distributions for EIR-like meta-molecules with a different substrate thickness d, in

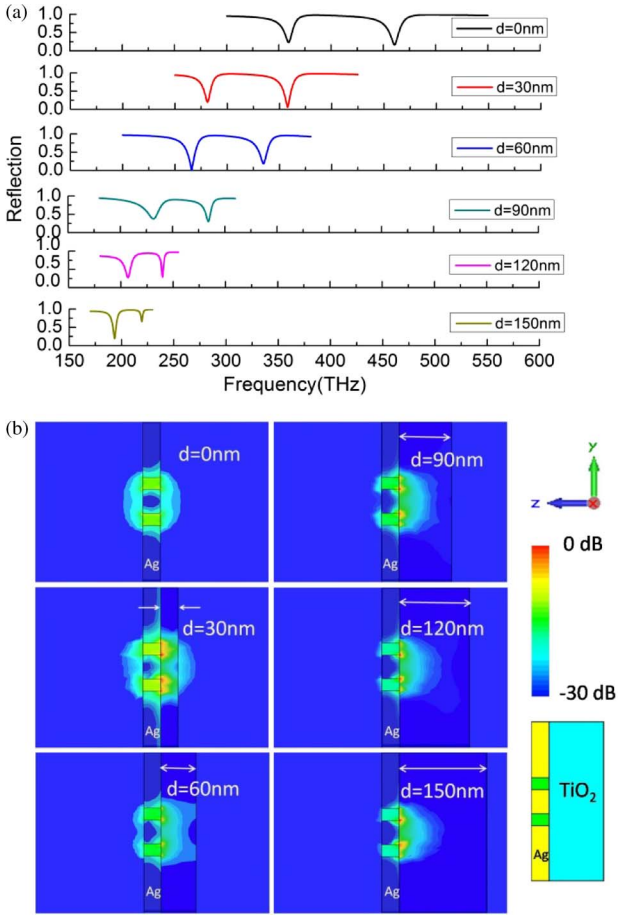

Fig. 4. (a) Reflection spectra and (b) the related EM field distributions of the EIR-like meta-molecules with different substrate thickness d. The frequencies of these distributions are chosen at the center frequencies of the EIR-like reflection window.

Fig. 4(b). The planes shown in Fig. 4(b) are cut along the dotted line and perpendicular to the x-axis shown in Fig. 3(a). It is clear that when the substrate thickness exceeds 90 nm, the EM field distributions of the local modes are almost unchanged. This explains the reason why the shifting rate of the EIR-like spectrum tends to decrease around the lower frequency range. In addition, the center frequency between the two dips of the EIR-like reflection spectra can be regarded as the ω_0 frequency defined in Eq. (3). At this frequency, the steep dispersion and related slow light effect give rise to the Q-factor enhancement of the OTS.

C. Simulation on Enhanced Lasing Enhancement

For the validation of lasing enhancement effect, a meta-surface-PC hetero-structure $MS(CD)_6$ is proposed, by coating an MS layer on a PC consisting of alternating SiO_2 (layer C) and TiO_2 (layer D) layers, as shown in Fig. 5(a). The refractive indices and thicknesses of TiO_2 and SiO_2 layers are $n_c = 1.46$, $n_D = 2.16$, $d_c = 260$ nm, and $d_D = 153$ nm, respectively. For comparison, an initial configuration of metal-PC hetero-structure, $M(CD)_6$, is also designed, with a 30 nm thick silver film deposited on PCs. Here, the metal layer is supposed

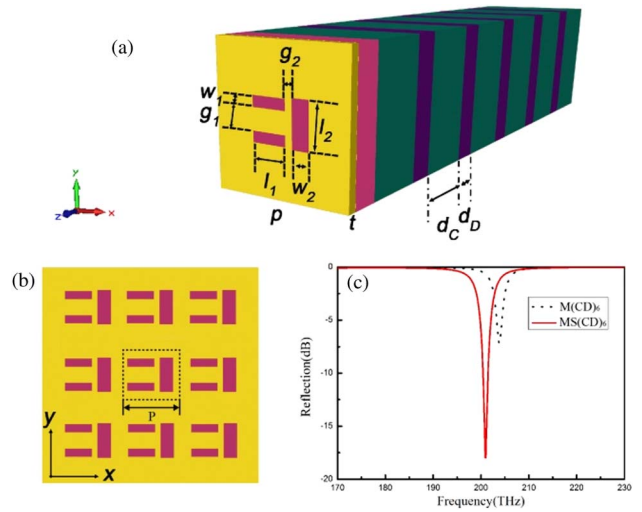

Fig. 5. (a) Schematic of the MS-PC hetero-structure. The geometry parameters are $l_1 = 100$ nm, $l_2 = 128$ nm, $w_1 = 30$ nm, $w_2 = 50$ nm, $g_1 = 60$ nm, $g_2 = 70$ nm and $d_C = 260$ nm, $d_D = 153$ nm, $P = 400$ nm, and $t = 30$ nm. The periods in both the x and the y directions are $P = 400$ nm. The thickness of the silver film on the PC substrate is $t = 30$ nm. (b) Front view of the meta-surface with EIR-like dispersion. (c) Reflection spectra for $M(\mathrm{CD})_6$ (black dotted line) and $\mathrm{MS(CD)}_6$ structures (red solid line).

to be Ag, with Drude-like dispersion [20]. As for the MS-PC hetero-structure, its concrete parameters are $l_1 = 100$ nm, $l_2 = 128$ nm, $w_1 = 30$ nm, $w_2 = 50$ nm, $g_1 = 60$ nm, $g_2 = 70$ nm and $d_c = 260$ nm, $d_D = 153$ nm, $P = 400$ nm, and $t = 30$ nm, as shown in Fig. 5(a). Here, the increased g_2 gives rise to the narrowing of an EIR-like spectrum and the related EM confinement of Tamm interface mode.

Three-dimensional FDTD simulations are performed in a Cartesian x-y-z coordinate system, with a TM-polarized wave (magnetic field H polarized along the y direction) normally incident from the right side of our structure. Thus, the reflection spectra of $M(\mathrm{CD})_6$ and $\mathrm{MS(CD)}_6$ hetero-structures are figured out in Fig. 5(c), showing clearly the enhanced OTS whose reflection and Q-factor are both optimized. Reflection dips belonging to OTS emerge for both two hetero-structures in the vicinity of 200 THz. Meanwhile, the corresponding Q-factor of $\mathrm{MS(CD)}_6$ is much larger than that of the $M(\mathrm{CD})_6$ structure by a factor of around 4 times.

As follows, gain medium is introduced to verify the enhancement effect of the MS-PC hetero-structure. For clear comparison, the following two cases are considered. In case 1, a complete thin metal layer is adopted to form the $M(\mathrm{CD})_6$ structure, and the nearest dielectric layer D, TiO_2 layer is replaced by the gain materials. (It should be noticed that the thickness of the gain layer is changed accordingly to maintain the original optical path.) In case 2, the original structure of photonic crystal $(\mathrm{CD})_6$ keeps unchanged, yet some gain media are embedded into the slots of an EIR-like meta-surface structure. Here, a four-level two-electron atomic system is employed to describe the time evolution of the population density of gain material [21,22], with rate equations written as follows:

$$\frac{dN_3}{dt} = -\frac{N_3}{\tau_{32}} - \frac{N_3}{\tau_{30}} + \frac{1}{\hbar\omega_a}\cdot\tilde{E}\cdot\frac{d\overline{P_a}}{dt}, \tag{4a}$$

$$\frac{dN_2}{dt} = \frac{N_3}{\tau_{32}} - \frac{N_2}{\tau_{21}} + \frac{1}{\hbar\omega_e}\cdot\tilde{E}\cdot\frac{d\overline{P_e}}{dt}, \tag{4b}$$

$$\frac{dN_1}{dt} = \frac{N_2}{\tau_{21}} - \frac{N_1}{\tau_{10}} + \frac{1}{\hbar\omega_e}\cdot\tilde{E}\cdot\frac{d\overline{P_e}}{dt}, \tag{4c}$$

$$\frac{dN_0}{dt} = \frac{N_3}{\tau_{30}} + \frac{N_1}{\tau_{10}} - \frac{1}{\hbar\omega_a}\cdot\tilde{E}\cdot\frac{d\overline{P_a}}{dt}, \tag{4d}$$

where $\tilde{E}$ represents the total electric field and $\overline{P_a}$ and $\overline{P_e}$ are the net macroscopic polarizations resulting from the transition between state 0 to state 3, and from state 2 to state 1, respectively. N_0 to N_3 are the population density of molecules from energy level 0 to 3, accordingly. τ_{xy} represents the lifetime of the transition between energy level x and y. The detailed gain material parameters used in our simulations are (1) $\omega_e = 1.26 \times 10^{15}$ and $\omega_a = 5.03 \times 10^{15}$, with damping coefficients $\gamma_a = \gamma_b = 1.0 \times 10^{13}$; (2) lifetimes: $\tau_{21} = \tau_{30} = 3.0 \times 10^{-10}$ s, $\tau_{32} = \tau_{10} = 1.0 \times 10^{-13}$ s; and (3) the initial population density: $N_0 = 5.0 \times 10^{23}$ m^{-3}.

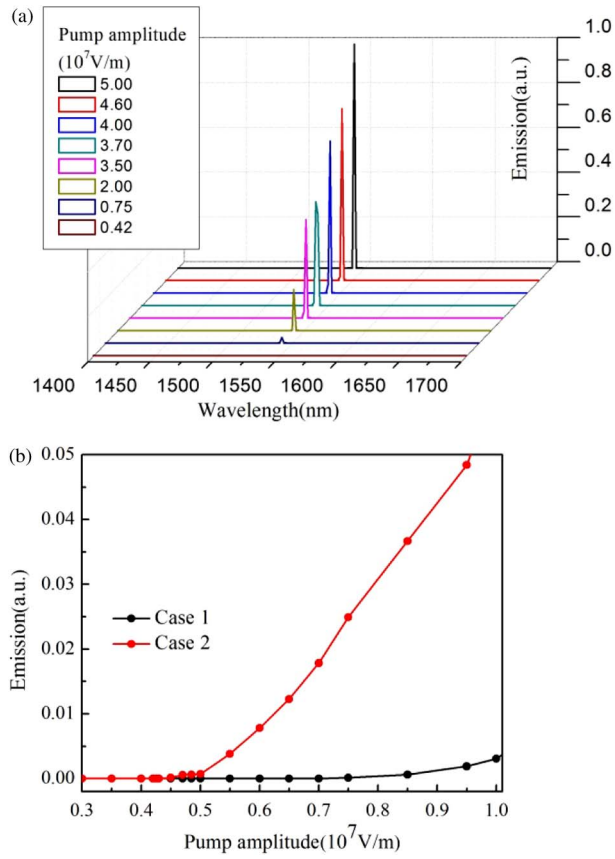

Fig. 6. (a) Emission spectra under different pump amplitudes in case 2. (b) The peak values of the simulated emission spectra as a function of the pump amplitudes. Black and red lines represent for case 1 and 2, respectively. Inset: details of (b).

When the above two structures with gain medium are pumped optically using an 800 nm picosecond-pulsed light, the emission spectra under different pump amplitudes are figured out as shown in Fig. 6(a).

It is clear that steep and narrow emitting spectra are observed, indicating the lasing effect at 1550 nm. By taking the peak values from spectra in Fig. 6(a), the max emission intensity as a function of the amplitude of the pump also is plotted in Fig. 6(b). Black and red lines represent the results for case 1 (M-PC with adjacent gain layer) and case 2 (MS-PC with embed gain medium in slots), respectively. For these two cases, the max emission intensity has the same trend. It is nearly zero below a certain threshold value; then it rises as the pump amplitude increases. Nevertheless, the threshold values and the max emission intensity in these two cases differ with each other obviously. The estimated threshold values for cases 1 and 2 are about 0.75×10^7 V/m and 0.43×10^6 V/m, respectively, showing clearly the threshold lowering effect. In the meantime, the enhancement of lasing action is exhibited clearly as the increase of pump amplitude.

3. CONCLUSION

In summary, the enhancement of the OTS and related lasing effect is investigated by introducing meta-surface with EIR-like dispersion. Numerical analysis and full-wave-simulation-based parameter retrieval method confirm that the structure-induced EIR-like dispersion gives rise to the Q-factor of OTS. As a result, an enhanced lasing effect also is verified when introducing a four-level two-electron atomic system. These features make our MS-PC structure promising to reduce the lasing threshold, enhance the fluorescence, and so on. Furthermore, this method only hires some surface etching procedures on the structure, which makes the fabrication much easier.

Funding. National Natural Science Foundation of China (NSFC) (11234010, 51377003, 51007064, 61137003).

Acknowledgment. The authors thank Yuan Li, and Zeyong Wei for their help in simulation.

REFERENCES

1. M. Kaliteevski, I. Iorsh, S. Brand, R. A. Abram, J. M. Chamberlain, A. V. Kavokin, and I. A. Shelykh, "Tamm plasmon-polaritons: possible electromagnetic states at the interface of a metal and a dielectric Bragg mirror," Phys. Rev. B **76**, 165415 (2007).
2. M. E. Sasin, R. P. Seisyan, M. A. Kalitteevski, S. Brand, R. A. Abram, J. M. Chamberlain, A. Y. Egorov, A. P. Vasil'ev, V. S. Mikhrin, and A. V. Kavokin, "Tamm plasmon polaritons: slow and spatially compact light," Appl. Phys. Lett. **92**, 251112 (2008).
3. C. Symonds, A. Lemaitre, E. Homeyer, J. C. Plenet, and J. Bellessa, "Emission of Tamm plasmon/exciton polaritons," Appl. Phys. Lett. **95**, 151114 (2009).
4. L. J. Dong, H. T. Jiang, H. Chen, and Y. L. Shi, "Enhancement of Faraday rotation effect in heterostructures with magnetoopticalmetals," J. Appl. Phys. **107**, 093101 (2010).
5. H. Lu, W. Li, C. H. Xue, H. T. Jiang, X. Y. Jiang, and H. Chen, "High-efficiency nonlinear platform with usage of metallic nonlinear susceptibility," Opt. Lett. **38**, 1283–1285 (2013).
6. C. H. Xue, H. T. Jiang, and H. Chen, "Nonlinear resonance-enhanced excitation of surface plasmon polaritons," Opt. Lett. **36**, 855–857 (2011).
7. A. Alù and N. Engheta, "Pairing an epsilon-negative slab with a mu negative slab: resonance, tunneling and transparency," IEEE Trans. Antennas Propag. **51**, 2558–2571 (2003).
8. O. Gazzano, S. M. de Vasconcellos, K. Gauthron, C. Symonds, J. Bloch, P. Voisin, J. Bellessa, A. Lemaitre, and P. Senellart, "Evidence for confined Tamm plasmon modes under metallic microdisks and application to the control of spontaneous optical emission," Phys. Rev. Lett. **107**, 247402 (2011).
9. H. Lu, Y. H. Li, T. H. Feng, S. H. Wang, C. H. Xue, X. B. Kang, G. Q. Du, H. T. Jiang, and H. Chen, "Optical Tamm states in heterostructures with highly dispersive planar plasmonic metamaterials," Appl. Phys. Lett. **102**, 111909 (2013).
10. Y. Zhao and A. Alu, "Manipulating light polarization with ultrathin plasmonic metasurfaces," Phys. Rev. B **84**, 205428 (2011).
11. X. B. Yin, Z. L. Ye, J. Rho, Y. Wang, and X. Zhang, "Photonic spin Hall effect at metasurfaces," Science **339**, 1405–1407 (2013).
12. L. L. Huang, X. Z. Chen, H. Mühlenbernd, H. Zhang, S. M. Chen, B. F. Bai, Q. F. Tan, G. F. Jin, K. W. Cheah, C. W. Qiu, J. Li, T. Zentgraf, and S. Zhang, "Three-dimensional optical holography using a plasmonic metasurface," Nat. Commun. **4**, 1–8 (2013).
13. S. E. Harris, J. E. Field, and A. Imamoglu, "Nonlinear optical processes using electromagnetically induced transparency," Phys. Rev. Lett. **64**, 1107–1110 (1990).
14. S. Zhang, D. A. Genov, Y. Wang, M. Liu, and X. Zhang, "Plasmon-induced transparency in metamaterials," Phys. Rev. Lett. **101**, 047401 (2008).
15. P. Tassin, L. Zhang, T. Koschny, E. N. Economou, and C. M. Soukoulis, "Low-loss metamaterials based on classical electromagnetically induced transparency," Phys. Rev. Lett. **102**, 053901 (2009).
16. N. Liu, T. Weiss, M. Mesch, L. Langguth, U. Eigenthaler, M. Hirscher, C. Sonnichsen, and H. Giessen, "Planar metamaterial analogue of electromagnetically induced transparency for plasmonic sensing," Nano Lett. **10**, 1103–1107 (2010).
17. J. Y. Guo, H. Chen, and H. Q. Li, "Effective permittivity and permeability of one-dimensional dielectric photonic crystal within a band gap," Chin. Phys. B. **17**, 2544–2552 (2008).
18. D. R. Smith, S. Schultz, P. Markoš, and C. M. Soukoulis, "Determination of effective permittivity and permeability of metamaterials from reflection and transmission coefficients," Phys. Rev. B **65**, 195104 (2002).
19. J. Y. Guo, Y. Sun, Y. W. Zhang, H. Q. Li, H. T. Jiang, and H. Chen, "Experimental investigation of interface states in photonic crystal heterostructures," Phys. Rev. E **78**, 026607 (2008).
20. M. A. Ordal, L. L. Long, R. J. Bell, S. E. Bell, R. R. Bell, R. W. Alexander, Jr., and C. A. Ward, "Optical properties of the metals Al, Co, Cu, Au, Fe, Pb, Ni, Pd, Pt, Ag, Ti, and W in the infrared and far infrared," Appl. Opt. **22**, 1099–1120 (1983).
21. S. H. Chang and A. Taflove, "Finite-difference time-domain model of lasing action in a four-level two-electron atomic system," Opt. Exp. **12**, 3827–3833 (2004).
22. A. Taflove, *Computational Electromagnetics: The Finite-Difference Time-Domain Method* (Artech House, 2005).